

W radiative decays and the determination of magnetic dipole and electric quadrupole moments of the W

Mark A. Samuel

Department of Physics, Oklahoma State University, Stillwater, Oklahoma 74078

Nita Sinha, Rahul Sinha, and M. K. Sundaresan

Ottawa-Carleton Institute for Physics, Carleton University, Ottawa, Canada K1S 5B6

(Received 3 December 1990)

The magnetic dipole moment of the W boson is given by $\mu = e(1 + \kappa + \lambda)/2M_W$ and its electric quadrupole moment is given by $Q = -e(\kappa - \lambda)/M_W^2$. A nonstandard magnetic dipole moment and a nonstandard electric quadrupole moment lead to different differential decay distributions in the radiative decays of W^\pm , $W^- \rightarrow e\bar{\nu}\gamma$ and $W^- \rightarrow d\bar{u}\gamma$. While hard photons are characteristic signatures of $\kappa \neq 1$ there is no such explicit signal for $\lambda \neq 0$. We present a technique for the determination of the values of κ and λ by measuring the total number of events in two regions of phase space. This experiment could be done at the CERN e^+e^- collider LEP II, where a clean source of W bosons will be available.

A few years ago it was discovered [1] by Mikaelian, Samuel, and Sahdev that the angular distribution for $d\bar{u} \rightarrow W^- \gamma$ ($u\bar{d} \rightarrow W^+ \gamma$) vanishes at a certain angle provided the magnetic moment of the W^\pm has the gauge theory value $\mu = e/M_W$. They proposed using this peculiar behavior in $p\bar{p}$ and pp collisions, $p\bar{p}$ or $pp \rightarrow W^\pm \gamma X$, where a dip persists, as a means of measuring the magnetic moment of the W . Subsequently it was shown [2] that these radiation amplitude zeros (RAZ's) are due to the complete destructive interference of the radiation patterns of the processes that contain one real photon, only like-sign charges, and $g=2$ for all particles with spin. These zeros are quite remarkable—the lowest-order amplitude vanishes for each spin state and the position of the zero is independent of photon energy.

Such zeros occur in a variety of processes, including the radiative W -boson decays $W^- \rightarrow d\bar{u}\gamma$ ($W^+ \rightarrow u\bar{d}\gamma$) and $W \rightarrow e\nu\gamma$, which we write as $W \rightarrow q_i\bar{q}_j\gamma$. Grose and Mikaelian [3] have shown that these processes have a RAZ if $g=2$ for the W . These previous calculations did not consider an electric quadrupole moment (EQM) for the W , which is included here. The most general CP -conserving $WW\gamma$ vertex is given by Kim and Tsai [4], and depends on the two parameters λ and κ . The standard-model (SM) values are $\lambda=0$ and $\kappa=1$. The electric quadrupole moment and magnetic dipole moment are given in terms of these parameters as

$$Q = \frac{-e(\kappa - \lambda)}{M_W^2} \quad (1)$$

and

$$\mu = \frac{e(1 + \kappa + \lambda)}{2M_W}, \quad (2)$$

respectively.

The previous calculations, referred to above, all assumed $\lambda=0$. For the SM values, $\kappa=1$ and $\lambda=0$, we have

$$Q = \frac{-e}{M_W^2}, \quad \mu = \frac{e}{2M_W}, \quad (3)$$

and the RAZ is preserved. An experiment to measure κ and λ could be done at the CERN e^+e^- collider at LEP II, where a clean source of W bosons will be available. It would be much more difficult at hadron colliders where the Dalitz plot would be contaminated by background events.

We shall consider the general case and allow κ and λ to vary from their SM values. Consider a general process

$$W^-(P) \rightarrow q_i(p_i) + \bar{q}_j(p_j) + \gamma(k), \quad (4)$$

where M_W , m_i , and m_j are the masses of W , q_i , and q_j , respectively, and P , p_i , and p_j are their respective four-momenta, and k is the photon four-momentum. The fermion electric charges are Q_i for q_i and Q_j for \bar{q}_j . In this paper we shall consider q_i, \bar{q}_j to be light quarks or leptons:

$$m_i/M_W \ll 1, \quad m_j/M_W \ll 1, \quad (5)$$

i.e., the massless limit. We choose to work with the variables [5]

$$X = \frac{2(p_i + p_j) \cdot k}{M_W^2}, \quad Y = \frac{(p_i - p_j) \cdot k}{(p_i + p_j) \cdot k}. \quad (6)$$

These are generalizations of the variables used by Samuel and Tupper [6] and have several advantages over the variables used in Ref. [3]. These variables are related to the conventional variables t and u by the simple relations

$$X = \frac{t + u}{M_W^2}, \quad Y = \frac{t - u}{t + u}. \quad (7)$$

The RAZ (for $\kappa=1$ and $\lambda=0$) occurs at

$$Y = \bar{Q} = \frac{Q_i - Q_j}{Q_i + Q_j}, \quad (8)$$

$$X = \frac{2E_\gamma}{M_W}. \quad (9)$$

which is independent of X or the fermion masses. Moreover in the W center-of-mass frame, X is simply the scaled photon energy:

The lowest-order partial differential decay rate in the massless case is

$$\frac{1}{\Gamma_0} \frac{\partial^2 \Gamma}{\partial X \partial Y} = \left[\frac{\alpha}{2\pi} \right] \left[Z^2 \left[\frac{1-X-X^2(1+Y^2)/4}{X(1-Y^2)} \right] - \eta Z \frac{XY}{4} + \eta^2 \frac{X}{16} \left[1-X + \frac{(1-Y^2)(1+X)}{2} \right] + \eta \lambda \frac{X(1-X)(3-Y^2)}{16} + \lambda^2 \frac{X(1-X)(2XY^2 - Y^2 - 2X + 3)}{32} \right], \quad (10)$$

where

$$\Gamma_0 = \frac{N_c \alpha M_W}{12 \sin^2 \theta_W} |V_{ij}|^2, \quad (11)$$

with the color factor $N_c = 3$ for the quark case and $N_c = 1$ for the lepton case, and the zero factor

$$Z = (Y - \bar{Q}); \quad (12)$$

V_{ij} is the Kobayashi-Maskawa (KM) matrix element and

$$\eta = \kappa - 1. \quad (13)$$

In the massless limit, the interference of λ and SM terms vanishes and the variables X and Y lie in the range

$$0 \leq X \leq 1, \quad -1 \leq Y \leq 1. \quad (14)$$

It can be seen explicitly from Eq. (10) that, for the SM values, $\eta = \lambda = 0$ the differential decay rate has an RAZ at $Z = 0$ or $Y = \bar{Q}$. Our results agree with the previous calculations [5,6] when $\lambda = 0$.

In the following we will present a way to determine κ

and λ , and, hence, the magnetic and quadrupole moments of the W boson, from radiative W decay measurements. We show the contributions of the various terms in Eq. (10) in the form of scatter plots in X and Y , where the density of the marks is proportional to the magnitude of each term. The scale used is such that the number of marks in each square of size $\Delta X = 0.1$ and $\Delta Y = 0.1$, divided by 300, equals $\partial^2 \Gamma / \partial X \partial Y$. We first consider the decay $W^+ \rightarrow u\bar{d}\gamma$. The RAZ for this process occurs at

$$Y = \bar{Q} = +\frac{1}{3}.$$

(For $W^- \rightarrow d\bar{u}\gamma$ it occurs at $Y = -\frac{1}{3}$.) Figure 1 shows the contributions from the SM² term [first term in Eq. (10)]. The RAZ at $Y = \frac{1}{3}$ is clearly seen. Figure 2 shows the contribution of the η^2 term, for $\eta = 9$. The coefficient of this term is large close to $X = 1$. Figure 3 shows the λ^2 contribution, for $\lambda = 10$. The coefficient of this term is significant in the range $0.2 \leq X \leq 0.7$. Figure 4 shows all the terms in Eq. (10). It can be seen that the separate terms are confined to separate parts of the scatter plot and can, in principle, be separated.

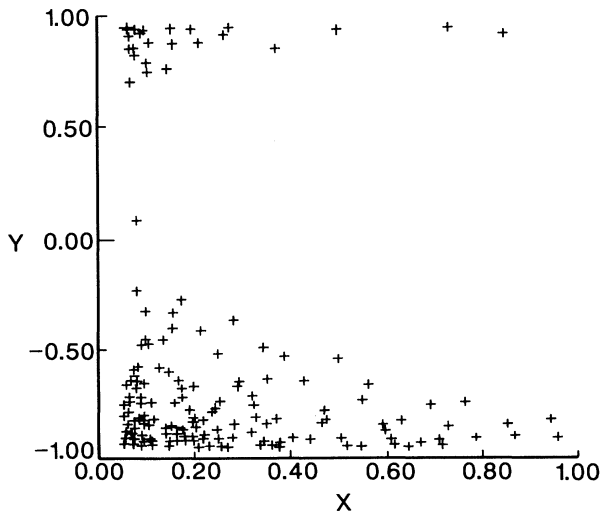


FIG. 1. Scatter plot for $W^+ \rightarrow u\bar{d}\gamma$ in X and Y for the SM² term.

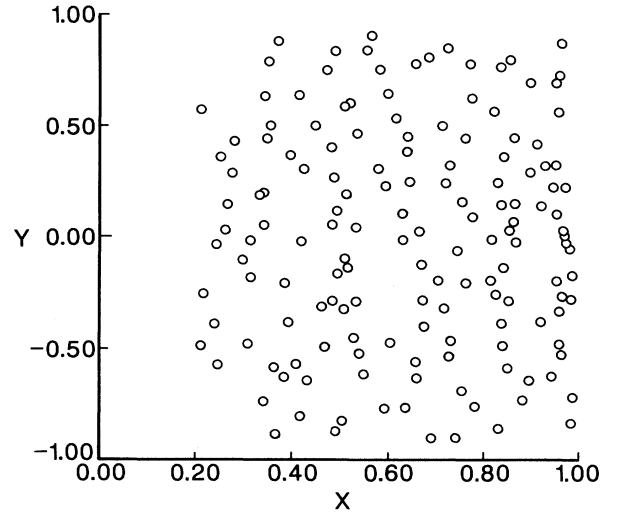


FIG. 2. Scatter plot for $W^+ \rightarrow u\bar{d}\gamma$ in X and Y for the η^2 term.

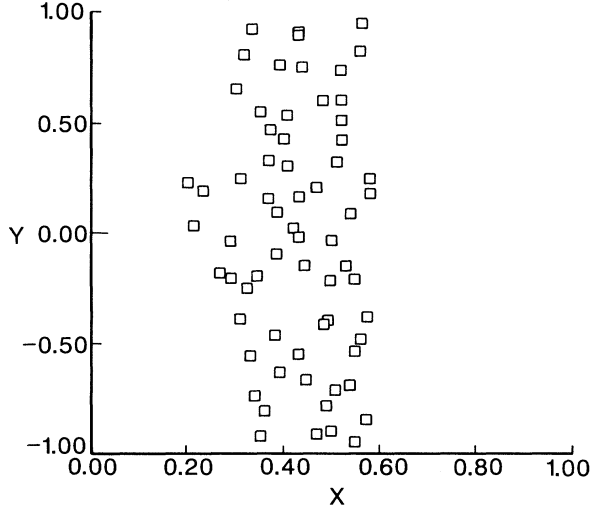


FIG. 3. Scatter plot for $W^+ \rightarrow u\bar{d}\gamma$ in X and Y for the λ^2 term.

For the decay $W^+ \rightarrow e^+\nu\gamma$ or $W^- \rightarrow e^-\nu\gamma$ the RAZ occurs at

$$Y = \bar{Q} = 1. \quad (15)$$

Figure 5 shows the SM^2 contribution. The RAZ at $Y = +1$ is clearly visible. Figure 6 shows the sum of all terms (i.e., total contribution). Again the separate terms are confined to separate parts of the scatter plot and can, in principle, be distinguished. The η^2 and λ^2 are the same as in the $W^+ \rightarrow u\bar{d}\gamma$ case, shown in Figs. 2 and 3, respectively.

Events with hard photons (i.e., $E \approx M_W/2$) come dominantly from the η^2 terms in Eq. (10). Such hard-photon

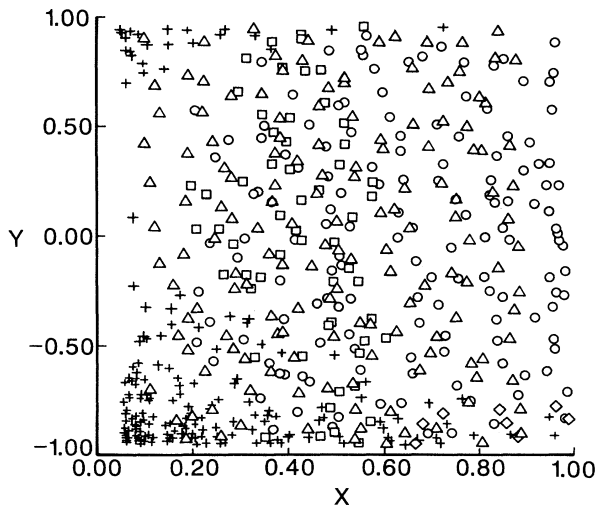


FIG. 4. Scatter plot for $W^+ \rightarrow u\bar{d}\gamma$ in X and Y for the sum of all the terms (total). The codes used are $\triangle\triangle\triangle\triangle$, $\eta\lambda$ interference; $\diamond\diamond\diamond\diamond$, ηSM interference; $\circ\circ\circ\circ$, η^2 ; $\square\square\square\square$, λ^2 ; $++++$, SM^2 .

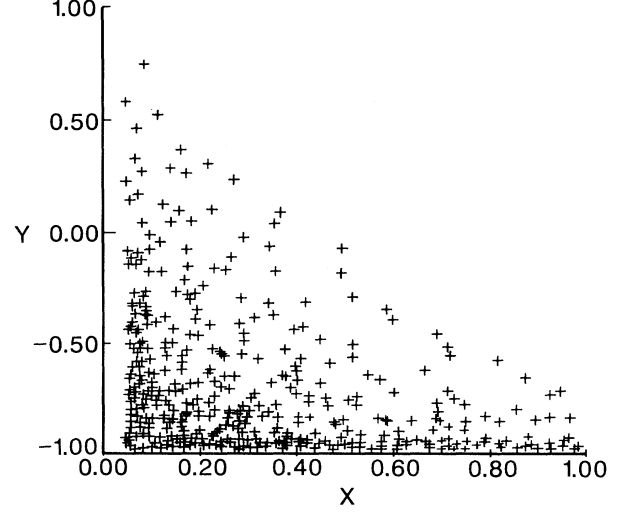


FIG. 5. Scatter plot for $W^+ \rightarrow e^+\nu\gamma$ in X and Y for the SM^2 term.

events are signatures of new physics—in particular, they would indicate $\eta \neq 0$ ($\kappa \neq 1$). Thus by cutting close to $X = 1$, the value of η can be determined as long as $\lambda \leq \eta$ (see Figs. 4 and 6). The absence of hard photons does not necessarily indicate that the W is a standard-model boson. A signature for $\lambda \neq 0$ is not so explicit, and its value much harder to extract. In the range of phase space where the λ^2 coefficient is most significant, there is also a sizable η - λ interference term, which does not allow a similar determination of the parameter λ .

We present below a technique for the determination of both η and λ , by estimation of the number of events in two separate regions of phase space. We integrate the

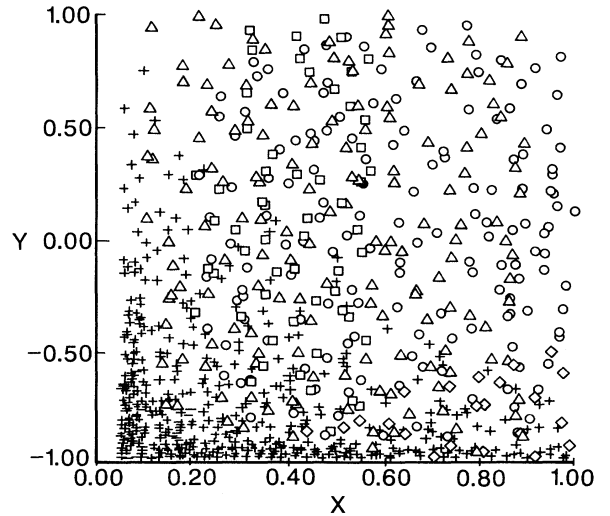


FIG. 6. Scatter plot for $W^+ \rightarrow e^+\nu\gamma$ in X and Y for the sum of all the terms (Total). The codes used are $\triangle\triangle\triangle\triangle$, $\eta\lambda$ interference; $\diamond\diamond\diamond\diamond$, ηSM interference; $\circ\circ\circ\circ$, η^2 ; $\square\square\square\square$, λ^2 ; $++++$, SM^2 .

differential width in Eq. (10) over two different regions of phase space, specified by cut I and cut II, and normalize it with respect to $\Gamma(W \rightarrow e\nu)$ to get the number of events n_I and n_{II} in the respective cut regions. In each case we get a quadratic form in η and λ , which results in an ellipse in the η - λ plane. Corresponding to the different number of events, we get a series of concentric ellipses.

In the leptonic decay mode $W \rightarrow e\nu\gamma$, we choose the two cuts as

$$\begin{aligned} \text{cut I, } E_e \geq 0.2 \text{ GeV, } E_\gamma \geq 5 \text{ GeV, } \theta_{e\gamma} \geq 5^\circ; \\ \text{cut II, } E_e \geq 0.2 \text{ GeV, } E_\gamma \geq 20 \text{ GeV, } \theta_{e\gamma} \geq 130^\circ; \end{aligned} \quad (16)$$

where E_e, E_γ are the electron and photon energies, and $\theta_{e\gamma}$ is the angle between the electron and the photon. Cut I is chosen to include almost the entire phase space, except the singular points in Eq. (10), and to account for the experimental resolutions. To reduce errors in determination of η and λ , cut II is optimized so that the angle between the major axis of the two sets of ellipses is maximized and yet there are enough (observable) events. The integrations in the above specified regions results in

$$\begin{aligned} n_I = NB \frac{\alpha}{2\pi} (168.5 + 7.45\eta^2 - 0.08\eta + 0.19\lambda^2 \\ + 0.53\eta\lambda) \times 10^{-1}, \\ n_{II} = NB \frac{\alpha}{2\pi} (15.54 + 7.27\eta^2 + 0.59\eta + 0.39\lambda^2 \\ + 1.21\eta\lambda) \times 10^{-2}, \end{aligned} \quad (17)$$

where $N = 100\,000$ is the total number of W 's produced and B is the branching ratio for $W^- \rightarrow e\bar{\nu}$ ($B = 0.11$). The ellipses corresponding to various values of n_I and n_{II} are plotted in Fig. 7, where the solid line ellipses corre-

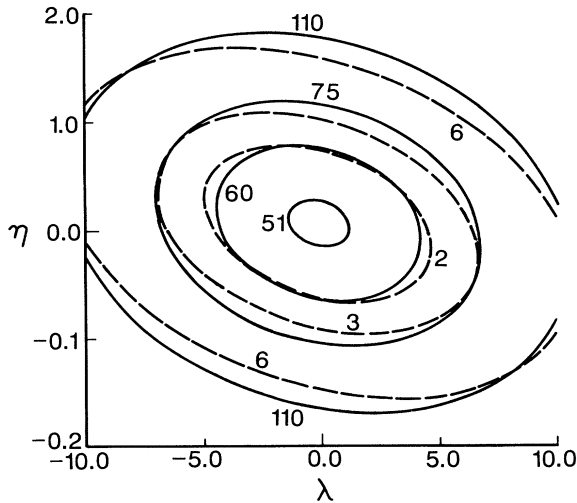


FIG. 7. Contours for number of events in the η - λ plane for $W \rightarrow e\nu\gamma$. The larger numbers correspond to ellipses with solid lines obtained from cut I, while the smaller numbers correspond to the dashed ellipses of cut II (see text for details).

spond to cut I, while the dashed ones to cut II. If η and λ are both zero, i.e., from SM alone, one finds $n_I = 215.3$. One would therefore expect a minimum of 216 events. Once the number of events n_I and n_{II} are measured the bounds on η and λ can be read off from Fig. 7. Further, the intersection points of the two sets of ellipses would yield exact solutions for η and λ . For example, the four points of intersection of the ellipses labeled 240 and 5 give the four possible values of η and λ :

- (i) $\eta = 1.44, \lambda = -7.15$,
- (ii) $\eta = -1.40, \lambda = -3.38$,
- (iii) $\eta = 1.48, \lambda = 2.43$,
- (iv) $\eta = -1.35, \lambda = 7.78$.

To narrow down the correct value from the four members of the set would require at least one more constraint equation of the type Eq. (17). We note that the values of η and λ determined would have a spread due to statistical errors in the number of events. Consider the interesting scenario where no events are observed in the cut II region. With 90% C.L. this means $n_{II} \leq 2.3$. This would yield the values $-0.66 \leq \eta \leq 0.60$ and $-2.72 \leq \lambda \leq 2.73$, allowing us to probe very close to the SM values.

A similar procedure is carried out for the quark decay mode. In this case we choose the cuts

$$\begin{aligned} \text{cut I, } E_q (E_{\bar{q}}) \geq 1 \text{ GeV, } \theta_{q\gamma} (\theta_{\bar{q}\gamma}) \geq 20^\circ, \\ \text{cut II, } E_q (E_{\bar{q}}) \geq 0.4M_W, \theta_{q\bar{q}} \geq 110^\circ, \end{aligned} \quad (18)$$

where $E_q (E_{\bar{q}})$ are the quark (antiquark) energies, $\theta_{q\gamma} (\theta_{\bar{q}\gamma})$ is the quark- (antiquark-) photon angle, and $\theta_{q\bar{q}}$ is the angle between q and \bar{q} . Again cut I includes almost

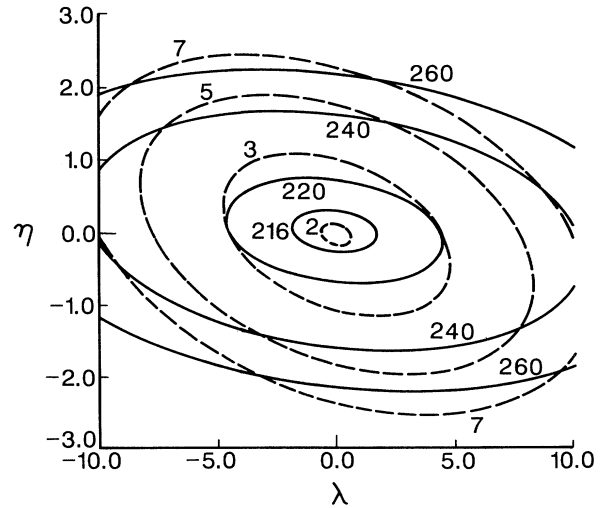


FIG. 8. Contours for number of events in the η - λ plane for $W^+ \rightarrow u\bar{d}\gamma$ and $W^- \rightarrow \bar{u}d\gamma$. The larger numbers correspond to ellipses with solid lines obtained from cut I, while the smaller numbers correspond to the dashed ellipses of cut II (see text for details).

the entire phase space, except the singular points and experimental resolutions. Here we cut at higher quark (antiquark) energies and quark- (antiquark-) photon angle due to restrictions on jet identification. These more stringent cuts result in substantial reduction in the number of events in comparison to the lepton case. We once again optimize cut II as in the lepton decay mode. The two cuts result in the following number of events:

$$\begin{aligned} n_{\text{I}} &= NB \frac{\alpha}{2\pi} (13.1 + 5.28\eta^2 - 0.63\eta + 0.14\lambda^2 \\ &\quad + 0.36\eta\lambda) \times 10^{-1}, \\ \eta_{\text{II}} &= NB \frac{\alpha}{2\pi} (2.63 + 5.50\eta^2 - 0.59\eta + 0.12\lambda^2 \\ &\quad + 0.52\eta\lambda) \times 10^{-2}, \end{aligned} \quad (19)$$

where B is the branching ratio for $W \rightarrow e\bar{\nu}$. The ellipses for $N = 100\,000$ are shown in Fig. 8.

We wish to emphasize that the *determination of the parameters η and λ does not require explicit identification of the up-type jet and down-type jet*, nor the distinction between the processes $W^+ \rightarrow u\bar{d}\gamma$ or $W^- \rightarrow \bar{u}d\gamma$. To ensure this, cuts on events required for measuring η and λ have to be symmetric in t and u ; the phase-space distribution of W^- events can be obtained from that of W^+ events by a $t \leftrightarrow u$ ($X \leftrightarrow -X$) exchange. To estimate η and

λ we only need to know jet energies and opening angles.

Finally we would like to comment on the experimental situation. In the case of the hadronic decay mode, the RAZ occurs in the interior of phase space ($Y = \frac{1}{3}$, for $W^+ \rightarrow u\bar{d}\gamma$), while for the leptonic decay mode it is on the edge of phase space ($Y = +1$, for $W^+ \rightarrow e^+\nu\gamma$). However, experimentally, the leptonic decay mode is cleaner. This experiment could be done at LEP II where a clean source of W bosons will be available via the reaction $e^+e^- \rightarrow W^+W^-$ and where the W 's are produced nearly at rest.

It will therefore be possible to test the W to see if it is really the SM W boson with $\kappa=1$ and $\lambda=0$ and to observe the RAZ's. Our aim here has been to present a general technique for determining the values of η and λ from the relatively smaller number of W 's produced (even without having the full spectrum). Some recent related work can be found in Ref. [7] and references therein.

One of us (M.A.S.) would like to thank Leon Lederman, Mark Timko, U. Baur, and Darryl Dibitonto for helpful discussions. This work was funded by the Natural Sciences and Engineering Research Council of Canada through Grant No. A1574. This work was also supported by the U.S. Department of Energy under Grant No. DE-FG05-85ER 40215.

-
- [1] K. O. Mikaelian, M. A. Samuel, and D. Sahdev, Phys. Rev. Lett. **43**, 746 (1979).
 [2] S. J. Brodsky and R. W. Brown, Phys. Rev. Lett. **49**, 996 (1982); R. W. Brown, K. Kowalski, and S. J. Brodsky, Phys. Rev. D **28**, 624 (1983); M. A. Samuel, *ibid.* **27**, 2724 (1983).
 [3] T. R. Grose and K. O. Mikaelian, Phys. Rev. D **23**, 123 (1981).
 [4] K. J. Kim and Y. S. Tsai, Phys. Rev. D **7**, 3710 (1973).
 [5] G. Tupper, J. Reid, G. Li, and M. A. Samuel, Phys. Lett. B **237**, 91 (1990).
 [6] M. A. Samuel and G. Tupper, Prog. Theor. Phys. Lett. **74**, 1352 (1985).
 [7] U. Baur and E. L. Berger, Phys. Rev. D **41**, 1476 (1990); U. Baur and D. Zeppenfeld, Nucl. Phys. **B308**, 127 (1988).